# EFFICIENT LIGHT CONFINEMENT TO λ/10 SPOT SIZES IN OPTICAL FIBRE

**M. Ding*, J.Y. Ou, N.P. Sessions, Y. Jung, G. Brambilla**

*University of Southampton, United Kingdom, E-mail: md20g09@orc.soton.ac.uk

**Keywords:** Optical fibre tip; surface plasmon polaritons; Focus Ion Beam

## Abstract

Light confinement beyond the diffraction limit has been achieved in optical fibre tips. We successfully fabricated a gold-coated optical fibre tip with wedge-shaped apex for the efficient excitation of surface plasmon polaritons (SPPs). An improved transmissivity higher than $10^{-2}$ and spot sizes of the order of λ/10 have been obtained by optimizing the overall light throughput along the fibre tip.

## 1 Introduction

Light confinement within a very small area is limited by diffraction and the minimum achievable spot size (ω) is related to the wavelength of the propagating light (λ) and to the refractive index (n) of the medium where light is being focused. The diffraction limit can be approximately expressed by the following expression [1]:

$$\omega \geq \frac{\lambda}{2n} \quad (1)$$

To overcome the diffraction limit, several different techniques have been used, including optical metamaterials [2-6], scanning near-field optical microscopy (SNOM) [7-11], and high index contrast waveguides [12,13]. Recently, metal-coated optical fibre tips exploiting surface plasmon polaritons (SPPs) have been proposed and experimentally demonstrated for efficient sub-wavelength light confinement. In 2007, Ding et al. [14] proposed an apertureless silver-coated optical tip in which the radially polarized waveguide modes of an optical fibre taper was converted into SPPs propagating at the outer surface of the tip. Although they are predicted to have extremely high transmission efficiencies, apertureless optical fibre tips with high transmission efficiency have never been realized. On the contrary, apertured tips have been widely used in the last decades, albeit without the aid of the SPPs [15-17]. Last year, apertured tips exploiting SPPs have been realized [18,19] to confine light to sub-wavelength spot sizes (λ/3) in optical fibres and optical fibre tips: the use of SPPs improved transmissivity by an order of magnitude. In this paper, both strong light confinement (~λ/10) and transmission efficiencies higher than $10^{-2}$ were successfully achieved using SPPs in optical fibre tips.

Fibre tips were precisely nanostructured using Focused Ion Beam (FIB) systems to convert light into SPPs and then back into light at the apex.

## 2 Device fabrication

Figure 1 shows the schematic diagram of the proposed device fabrication process. The fabrication process can be divided into four main steps: (a) manufacture of an optical fibre tip, (b) tip milling using FIB system, (c) deposition of a thin gold layer onto the optical fibre tip, and (d) opening an extremely small aperture at the coated fibre tip apex.

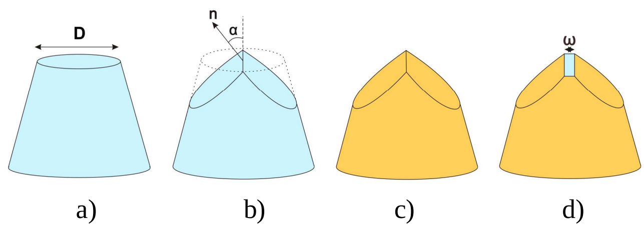


Figure 1. Schematic of device fabrication. a) an optical fibre (CORNING-SMF28) tip was manufactured by P-2000 micropipette puller, D is the tip diameter; b) the tip was milled by a Focused Ion Beam (FIB) system at a specific angle α; c) a thin layer of gold was deposited; d) an extremely small aperture with size ω was opened at the tip using the FIB system.

### 2.1 Tip manufacture

First, a fibre tip was manufactured using a commercial micropipette puller (P-2000) which is $CO_2$ laser pulling machine controlled by a microprocessor. The default configuration of the P-2000 allows for the fabrication of fibre tips with exceedingly small diameters. Typically, fibres can be pulled from 125μm down to 40nm diameters and have a taper length of about 1mm.

Since high transmission efficiencies are targeted in this paper, the taper angle of the optical fibre tip has to be small enough to adiabatically convert the fundamental mode in the fibre core into a fundamental mode guided by the cladding/air interface. The taper profile is called adiabatic when the light launched into a taper propagates in the same mode, without any power transfer to other modes. J. D. Love proposed a criterion for adiabaticity [20]: if the local taper length is larger than the coupling length between the fundamental mode and the dominant coupling mode, power loss will be minimized and the tip is adiabatic. The adiabatic angle can be described as a function of the propagation constants of two lowest modes ($\beta_1$ and $\beta_2$) and of the local radius (r) of the guiding structure:

$$\overline{\Omega} = \frac{r(\beta_1 - \beta_2)}{2\pi} \quad (2)$$

If the taper angle $\Omega < \overline{\Omega}$, tapers are adiabatic, while for $\Omega \geq \overline{\Omega}$, the tapers are non-adiabatic. Transmission larger than 98% can be obtained in adiabatic fibre tapers [21,22].

### 2.2 Nanostructuring

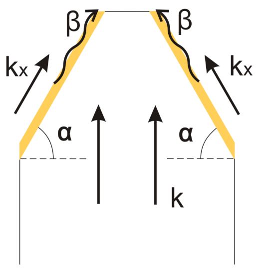


Figure 2. Schemetic of designed structure. $\alpha$ presents the resonance angle. $\beta$, k and $k_x$ represent the propagation constant of the SPPs, the wave vector of light and its component along $\beta$ respectively.

The adiabatic fibre tip was nanostructured to a wedge-shape using the FIB system: two surfaces were cut with the same slope (within the instrument resolution). The angle $\alpha$ was chosen to optimize the SPPs excitation at the tip. SPPs can be described as free electron oscillations in metals and can be excited when transversely magnetic polarized beams hit the interface between metal and dielectric at a specific resonance angle $\alpha$.

Resonance occurs when the projection of the light wave vector on the newly formed surface $k_x = k \cdot \sin\alpha$ equals the SPPs propagation constant $\beta$ in the same direction (fig. 2). The resonance angle condition can be expressed as:

$$\alpha = \arcsin\left(\frac{1}{n_{eff}}\sqrt{\frac{\varepsilon_{gold}\varepsilon_{air}}{\varepsilon_{gold} + \varepsilon_{air}}}\right). \quad (3)$$

where the $n_{eff}$ is the fundamental mode ($HE_{11}$) effective index, and $\varepsilon_{gold}$ and $\varepsilon_{air}$ are the dielectric constants of gold and air, respectively. The dependence of the resonance angle on the wavelength is shown in fig. 3 for two different tip diameters.

Fig. 3 shows that $\alpha$ varies more than 10° in the range of wavelengths 600-1600nm and the smaller tip diameter presents a stronger dependence on the wavelength. Therefore, in tips not only the wavelength but also the tip diameter can be used to fulfill the resonance condition. In our experiments tips with D~1µm were chosen because they provide a better tolerance to nanostructuring imprecision: since the FIB accuracy can be higher than 0.1°, in tips with small diameters a small imprecision (0.1°) in $\alpha$ results in a shift of the resonance peak wavelength smaller than 100nm.

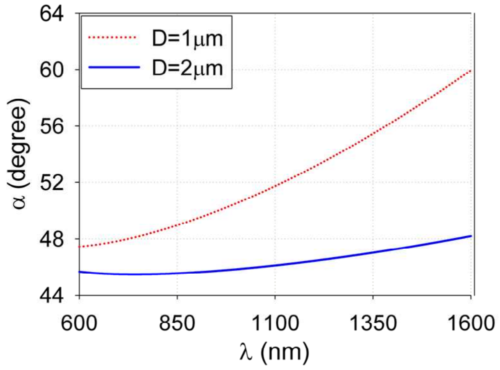


Figure 3. Dependence of the resonance angle $\alpha$ on the wavelength $\lambda$ for optical fibre tips with diameters D=1µm (red curve) and D=2µm (blue curve).

Fig. 4 shows SEM images of a nanostructured tip. The tip was firstly measured and then milled at the resonance angle $\alpha$ with a FIB system (fig. 4a). A ~30nm thick gold layer was deposited on the tip to excite SPPs and to avoid charging during processing; in fact, charge accumulation seriously degrades the FIB imaging and processing capabilities and makes the accurate thickness evaluation difficult. An extremely small aperture was finally opened at the tip apex (fig. 4b).

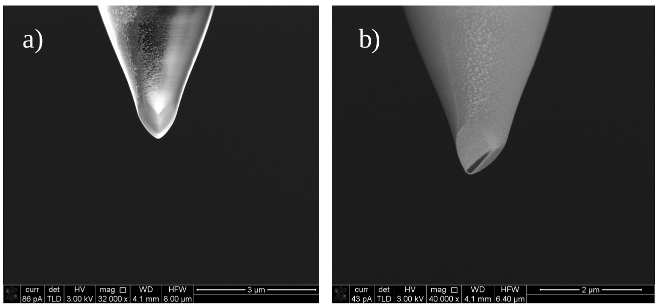


Figure 4. SEM images of a nanostructured tip. a) the tip was cut at resonance angle $\alpha$, b) an aperture (dark region) was opened at the apex of the gold coated tip. The tip diameter and the aperture size were 906nm and 80nm, respectively.

## 3 Experiment

To characterize the SPPs contribution to the sample transmissivity, the set-up shown in fig. 5 was used.

A supercontinuum (SC) source (Fianium Ltd, U.K.) delivers light over a very broad range of wavelengths (450-1800nm) with maximum pulse energy of 50nJ. The fiberized output is angle cleaved to avoid back reflections. Light from the SC source is launched into the modal filter [21] which eliminates high order modes. A polarization rotator designed by OZ Optics is used to control the input beam state of polarization. Light from the polarization rotator is then launched into samples, where it is firstly converted into the SPPs at the nanostructured surface and then converted back into light. Collection of the transmitted light is carried out using a multimodal optical fibre pigtail and an optical spectrum analyzer (OSA). Two XYZ stages are used to align the different fibre components.

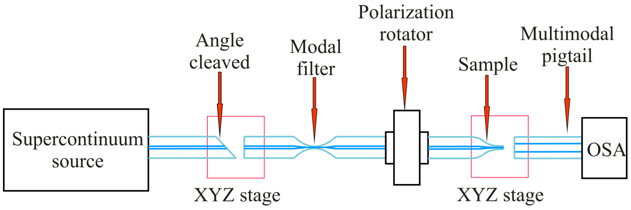


Figure 5. Schematic of the set-up used to characterize sample transmission

Measurements were carried out as follows: firstly, the set-up spectral response was recorded without any sample to provide a normalization base for the following spectra and to remove any wavelength dependence related to the source and to the modal filter. Next, the polarization angle was optimized to find maximum transmission. Finally, sample spectra were recorded. Measurements were carried out both in dry and in humid environments to verify that transmission was really aided by SPPs. In fact, SPP excitation and propagation conditions depend on the surrounding environment properties and a humidity change should result in a change of the amount of SPPs excited and propagating at a given interface. The sample had α~50°, resulting in a SPP resonance wavelength of 800nm.

## 4 Results

Fig. 6 summarizes the measurement results. Fig. 6a shows the spectral response of the set-up including SC source and modal filter. Figs. 6b and 6c present the spectra of the sample in dry and humid environments, respectively. Fig. 6d displays the normalized spectra in dry (red) and humid (blue) environments evaluated from the ratio between the spectra in fig. 6b and in fig. 6a and between the spectra in fig. 6c and in fig. 6a respectively. In humid environment, the transmissivity is reduced because of the change in the resonance condition. The increased attenuation in the spectrum recorded in humid environment cannot be ascribed to misalignments because the peak recovery time when the environment is dried up is not instantaneous, but occurs over a time span of several seconds. In addition, the tip has been exposed to a gentle blow of dry air and no transmission change was recorded. The normalized graphs of fig. 6d show a peak with ~3% transmissivity at a wavelength ~800nm, which coincides with the designed specifications. As a consequence, the SPPs are held responsible for the enhanced transmission. The high periodical noise in the normalized spectra is possibly caused by modal interference coming from the non-perfect adiabaticity of the tip profile; the small periodicity noise is probably due to the interference generated at air gaps between the optical components. This transmission efficiency is several orders of magnitude larger than that observed in common SNOM tips. The spot size of this sample is approximately λ/10. Smaller spot sizes can be envisaged if the aperture diameter decreases.

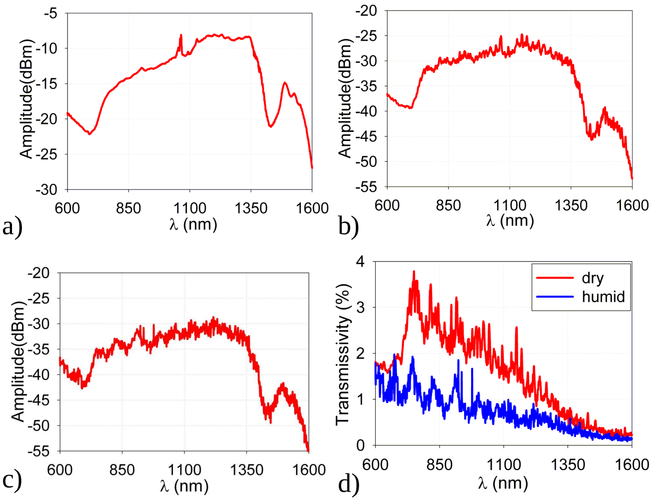


Figure 6. Measurement results. a) spectrum of the SC source, b) spectrum of the sample in dry environment, c) spectrum of the sample in humid environment, d) normalized transmission of the sample in dry and humid environments.

## 5 Conclusion

In conclusion, sub-wavelength light confinement to λ/10 with high transmission efficiency (higher than $10^{-2}$) was successfully achieved by exploiting surface plasmon polaritons at the apex of an optical fibre tip. Effective confinement to considerably smaller spot sizes can be predicted by decreasing the aperture size; surface plasmon polaritons dispersion will constitute a considerable limitation when nm size spot-sizes are approached.

## Acknowledgements

GB gratefully acknowledges the Royal Society (London, U.K.) for his University Research Fellowship.

## References

[1] M. Born and E. Wolf, *Principle of Optics*, ed., New York: Springer, pp. 461-464, (1999).

[2] V. Veselago, “Electrodynamics of substance with simultaneously negative electrical and magnetical permeabilites,” *Sov. Phys. Usp*., **volume**.10, pp. 509-514, (1968).

[3] J. B. Pendry, “Negative refraction makes a perfect lens,” *Phys. Rev. Lett*., **volume**. 85, pp. 3966-3969, (2000).

[4] M. Bayindir, K. Aydin, E. Ozbay, P. Markos, and C. M. Soukoulis, “Transmission properties of composite metamaterials in free space, ” *Appl. Phys. Lett*., **volume**. 81, pp. 120–122, (2002).

[5] T. Thomas, K. Dmitriy, U. Yaroslav, S. Gennady, and H. Rainer, “Near-field microscopy through a SiC superlens,” *Science*, **volume**. 313, pp. 1595, (2006).

[6] X. Zhang and Z. Liu, “Superlenses to overcome the diffraction limit, ” *Nat. Mater*., **volume**. 7, pp. 435-441, (2008).

[7] E. Betzig and J. K. Trautman, “Near-field optics: Microscopy, spectroscopy, and surface modification beyond the diffraction limit,” *Science*, **volume**. 257, pp.189-195, (1992).

[8] Y. Inouye and S. Kawata, “Near-field scanning optical microscope with a metallic probe tip,” *Opt. Lett*., **volume**. 19, pp. 159-161, (1994).

[9] H. Heinzelmann and D. W. Pohl, “Scanning near-field optical microscopy”, *Appl. Phys. A: Mater. Sci. Process*., **volume**. 59, pp. 89-101, (1994).

[10] F. Keilmann and R. Hillenbrand, “Near-field microscopy by elastic light scattering from a tip,” *Phil. Trans. R. Soc. Lond. A*, **volume**. 362, pp. 787-797, (2004).

[11] L. Novotny and S. J. Stranick, “Near-field optical microscopy and spectroscopy with pointed probes,” *Ann. Rev. Phys. Chem.*, **volume**. 57, pp. 303-331, (2006).

[12] Q. Xu, V. R. Almeida, R. R. Panepucci, and M. Lipson, “Experimental demonstration of guiding and confining light in nanometer-size low-refractive-index material,” *Opt. Lett*., **volume**. 29, pp.1626-1628, (2004).

[13] G. S. Wiederhecker, C. M. B. Cordeiro, F. Couny, F. Benabid, S. A. Maier, J. C. Knight, C. H. B. Cruz, and H. L. Fragnito, “Field enhancement within an optical fibre with a subwavelength air core,” *Nat. Photon*., **volume**. 1, pp. 115-118, (2007).

[14] W. Ding, S. R. Andrews, and S. A. Maier, “Internal excitation and superfocusing of surface plasmon polaritons on a silver-coated optical fiber tip,” *Phys. Rev. A*., **volume**. 72, pp. 063822.1- 063822.10, (2007).

[15] L. Novotny, D. W. Pohl, and P. Regli, “Light propagation through nanometer-sized structures:the two-dimensional-aperture scanning near- field optical microscope,” *J. Opt. Soc. Am. A*, **volume**. 11, pp. 1768–1779, (1994).

[16] J. A. Veerman, A. M. Otter, L. Kuipers, and N. F. van Hulst, “High definition aperture probes for near-field optical microscopy fabricated by focused ion beam milling,” *App. Phys. Lett*., **volume**. 72, pp. 3115-3117, (1998).

[17] B. Hecht, B. Sick, U. P. Wild, V. Deckert, R. Zenobi, O. J. F. Martin, and D. W. Pohl, “Scanning near-field optical microscopy with aperture probes: Fundamentals and applications,” *J. Chem. Phys.*, **volume**. 112, pp. 7761-7774, (2000).

[18] F. Renna, G. Brambilla, and David C. Cox, “Light confinement in optical fibers using surface plasmon polaritons,” *Photon. Technol. Lett.*, **volume**. 21, pp. 1508-1510, (2009).

[19] F. Renna, D. Cox, and G. Brambilla, “Effcient sub-wavelength ligth confinement using surface plasmon polaritons in tapered fibers,” *Opt. Express*, **volume**. 17, pp. 7658-7663, (2009).

[20] J. D. Love, W. M. Henry, W. J. Stewart, R. J. black, S. Lacroix, and F. Gonthier, “Tapered single-mode fibres and devices (Part 1: Adiabaticity criteria),” *IEE Proceedings J. Optoelectronics*, **volume**. 138, pp. 343-345, (1991).

[21] Y. Jung, G. Brambilla, and D.J. Richardson, "Broadband single-mode operation of standard optical fibers by using a sub-wavelength optical wire filter," *Opt. Express*, **volume**. 16, pp. 14661-14667, (2008).

[22] B. Hecht, B. Sick, U. P. Wild, V. Deckert, R. Zenobi, O. J. F. Martin, and D. W. Pohl, “Scanning near-field optical microscopy with aperture probes: Fundamentals and applications,” *J. Chem. Phys.*, **volume**. 112, pp. 7761–7774, (2000).